ISSN 1995-0780, Nanotechnologies in Russia, 2019, Vol. 14, Nos. 9–10, pp. 427–434. © Pleiades Publishing, Ltd., 2019.
Russian Text © The Author(s), 2019, published in Rossiiskie Nanotekhnologii, 2019, Vol. 14, Nos. 9–10.

SELF-ASSEMBLED STRUCTURES AND NANOASSEMBLIES

3D Structures Based on Reduced Graphite Oxide and Gold Nanoparticles and Their Sorption Properties

E. A. Eremina[a,*], A. Dobrovolskii[a], I. A. Lemesh[a], V. V. Eremin[a], A. V. Grigorieva[a], and E. A. Goodilin[a]

[a] *Moscow State University, Moscow, Russia*

**e-mail: ea_er@mail.ru*

Received December 3, 2019; revised January 29, 2020; accepted February 12, 2020

Abstract—The preparation of hydro- and aerogels based on reduced graphite oxide and gold nanoparticles obtained by the method of Turkevich is described. According to the transmission electron microscopy data, gold nanoparticles have a spherical shape and an average size of 16–18 nm. Sorption of methylene blue dye from water solutions was used to characterize the obtained 3D structures. The sorption properties of hydro- and aerogels were compared; it was shown that aerogels sorb the dye more efficiently (>80%) than a composite based on hydrogel (~50%). The formed porous 3D structure of the aerogel efficiently sorbs the molecules of the dye, while the gold nanoparticles facilitate its destruction under the visible light. Sorption by aerogels of pure graphite oxide is most efficient at room temperature, in a neutral medium, and in the absence of additional reducing agents. Introduction of gold nanoparticles to aerogels led to an increase of the maximal sorption by 15%.

DOI: 10.1134/S1995078019050045

INTRODUCTION

The currently studied structures based on graphene (graphene, graphene oxide, graphite oxide, and reduced graphite oxide) are "*smart*" objects; by modifying them one can purposefully create materials with various functional properties [1–4]. *Graphite oxide* is produced under the action of oxidizing agents ($KClO_3$, the Brodie method [5]; $KMnO_4$, the Hammers method [6, 7]; etc.) on graphite, which results in partial destruction of π bonds between graphite layers and the formation of various functional oxygen-containing groups (C=O, C–OH, C–O–C, and CO–OH) on the surface of carbon-containing layers. As a result of the oxidation process, the carbon layers are moved apart and separated from each other; cavities are formed between them, into which extraneous molecules can be sorbed.

The largest interlayer space is typical for 3D structures based on graphite oxide, which include hydro- and aerogels based on graphite oxide: in a hydrogel, the water content is more than 90 wt %, while in an aerogel water is practically absent. Aerogels are characterized by a density of the order of 2.4–4.0 mg/cm^3.

Methods for producing hydrogels based on graphite oxide can be divided into two main groups. The first one uses chemical reduction with ascorbic acid, iodides and hydroiodic acid, hydrazine, sulfides and sulfites of alkali metals, etc., the second uses the hydrothermal method, which is carried out in an autoclave at temperatures of 140–150°C [8–17]. It is proposed to use the method of cryochemical drying to obtain aerogels. Gold nanoparticles can be embedded in 3D structures based on graphite oxide, which allows amplification of the signal from sorbed molecules [18–21].

Russian chemists from the Kurnakov Institute of General and Inorganic Chemistry, RAS made a significant contribution to the development of methods for producing hydro- and aerogels based on graphene and composites with noble metal nanoparticles. The authors developed a new method for depositing platinum, palladium, and rhodium nanoparticles on the graphene surface by reducing in an autoclave a suspension of noble metal nanoparticles and graphene oxide in supercritical isopropanol [22, 23].

To assess the sorption properties of 3D structures based on graphene and its derivatives, dyes can be used that are used in the manufacture of textile and paper products and are dangerous pollutants. Dyes have complex aromatic structures and xenobiotic properties; therefore, their sorption from aqueous solutions and further destruction can be used for wastewater treatment [24].

The aim of this work was to synthesize composites based on 3D graphene structures and gold nanoparticles and study their sorption properties. 3D structures were formed in the form of hydro- and aerogels. Methylene blue, an organic dye intensively used for dyeing cotton, wool, and paper, which has a negative effect on the human body, was used as a model dye to

Fig. 1. (Color online) A sample of the rGO–AuNPs hydrogel and the remaining solution from the autoclave.

assess the effectiveness of sorption by 3D structures. The sorption properties of hydro- and aerogels were compared and the dependence of the efficiency of sorption by aerogels on various factors, that is, sorbent mass, acidity of the medium, temperature, and the presence of reducing agents, was studied.

MATERIALS AND METHODS

Reagents. Thermally expanded graphite, $KMnO_4$ (analytical grade), H_2SO_4 (concentrated, reagent grade), H_3PO_4 (85%, reagent grade), H_2O_2 (37%), sodium citrate $Na_3C_6H_5O_7$ (analytical grade), H_2O (distilled), C_2H_5OH (Ferein, 95%), $H_2C_2O_4$ (high-purity grade), $HAuCl_4$ solution (0.053 M), and sodium borohydride (analytical grade, Sigma Aldrich) were used as the starting reagents.

Obtaining graphite oxide. The synthesis of graphite oxide was carried out according to the procedure [7] using thermally expanded graphite, concentrated sulfuric and phosphoric acids.

The resulting graphite oxide emulsion was subjected to repeated washing and centrifugation until the pH of the supernatant was 6–7.

The synthesis process of graphite oxide can be described by the following conventional schemes:

$$G + H_2SO_4 + KMnO_4 = GO + K_2SO_4 + \text{red(Mn)} \text{ (in the presence of } H_3PO_4),$$

where G is graphite, GO is graphite oxide, red(Mn) is a mixture of reduced forms of manganese: Mn^{2+}, MnO_4^{2-}, and MnO_2,

$$GO + \text{red(Mn)} + H_2C_2O_4 + H_2O_2 = rGO + Mn^{2+} + CO_2 + H_2O + O_2,$$

where rGO is reduced graphite oxide. The concentration of GO in the resulting solutions was 2 mg/mL. The graphite oxide concentration was determined by weighing aliquots of a fixed volume solution.

Obtaining gold nanoparticles (AuNPs). The synthesis of gold nanoparticles was carried out according to the Turkevich method [25]. First, 50 mL of water were added to 300 μL of a 0.05 M $HAuCl_4$ solution, brought to a boil, and 1.5 mL of sodium citrate (Na_3Cit) solution was added. Heating was stopped after 10 min; the solution turned ruby red. The process proceeded according to the equation

$$2HAuCl_4 + 3Na_3C_6H_5O_7 = 2Au + 3Na_2C_5H_4O_5 + 3CO_2 + 3NaCl + 5HCl.$$

One mL of the obtained solution of gold nanoparticles contains 3.2×10^{-7} mol of gold.

Obtaining a hydro- and aerogel based on graphite oxide and gold nanoparticles. A hydrogel based on graphite oxide and gold nanoparticles was obtained using a solution of previously prepared gold nanoparticles: 4.8 mL of a graphite oxide solution (2 mg/mL) were mixed with a solution of prepared gold nanoparticles with a volume of 17.5 mL. The mixture was stirred on a magnetic stirrer for 20 min without heating, then 35 mg of ascorbic acid were added over 10 min and stirring was continued for 10 min. As a result, a solution of the "reduced graphite oxide–gold" nanocomposite was obtained, which was used to obtain hydro- and aerogel.

To obtain a hydrogel, the solution was placed in an autoclave for 12 h at a temperature of 140°C; the obtained product was a black "elastic" cylinder with a diameter of 2 cm and a height of 1.5 cm (Fig. 1). The color of the solution indicates the presence of unreacted gold nanoparticles.

For the synthesis of aerogels, samples of solutions of the individual reduced graphite oxide and reduced graphite oxide–gold were freeze dried on a Labconco 7948030 freeze dryer (United States) at a pressure of 0.7 mbar in the temperature range of –20 to +20°C.

RESEARCH METHODS

Optical absorption spectra were recorded on a Perkin-Elmer Lambda 950 UV/Vis/NearIR-range scanning spectrophotometer (Perkin-Elmer, United States).

Electron diffraction analysis and a detailed study of the microstructure were performed by transmission electron microscopy (TEM) using a LEO 912 AB Omega microscope with a LaB_6 cathode with an accelerating voltage of 100 kV (Carl Zeiss, Germany). When recording electron diffraction, the camera length was 265 mm; the standard was metallic gold.

X-ray phase analysis was performed using a Rigaku D/MAX 2500 diffractometer (Rigaku, Japan) with a Bragg–Brentano geometry with a rotating anode (CuK_α radiation). The registration was carried out step by step in the interval of angles $2\theta = 2°–80°$ with a step of 0.02° in 2θ at an exposure of 2 s per point. Processing of the obtained data was carried out using standard WinXpow software packages.

Raman-scattering spectroscopy (RS) studies were performed using an InVia Reflex microscope (Renishaw, England) in confocal mode using a red (He/Ne, wavelength, 632.8 nm, 20 mW) and a green laser (Ar, wavelength, 514.4 nm, 20 mW). The power of the neutral density filter for RS spectra was 100%. The signal accumulation time was 10 s. Alignment of the device was carried out using single-crystal silicon wafers as a standard. Spectra were recorded in the 100–3200 cm^{-1} range. Laser power was controlled using light-absorbing filters on the optical path.

RESULTS AND DISCUSSION

The results of X-ray phase analysis of all graphite-based samples are presented in Fig. 2. The X-ray diffraction pattern of the initial graphite contains an 002 reflection corresponding to an interplanar distance of 3.4 Å, which is consistent with the data for graphite presented in the [PCPDF] database, card 75-1621.

The X-ray diffraction pattern of the synthesized graphite oxide exhibits a wide reflex at $2\theta = 10.34°$ (interplanar distance 8.34 Å). The increase in interplanar distance compared to pure graphite is due to the oxidation of individual carbon layers and the formation of oxygen-containing functional groups, which contribute to the delamination of the carbon material. The absence of the 002 reflection in the X-ray diffraction pattern of the graphite oxide powder indicates the absence of the initial graphite. In addition, the wide reflex is observed in the diffractogram at $2\theta = 19.5°$, which indicates incomplete oxidation of the initial graphite. The X-ray diffraction pattern of reduced graphite oxide obtained in an autoclave shows an increase in the intensity of the reflection at $2\theta = 21°$ and the absence of reflections in the region of small angles corresponding to oxidized graphite oxide. These results indicate the reduction of some oxygen-containing functional groups, which results in a decrease in the interplanar distance of the sample to a value of 4.30 Å.

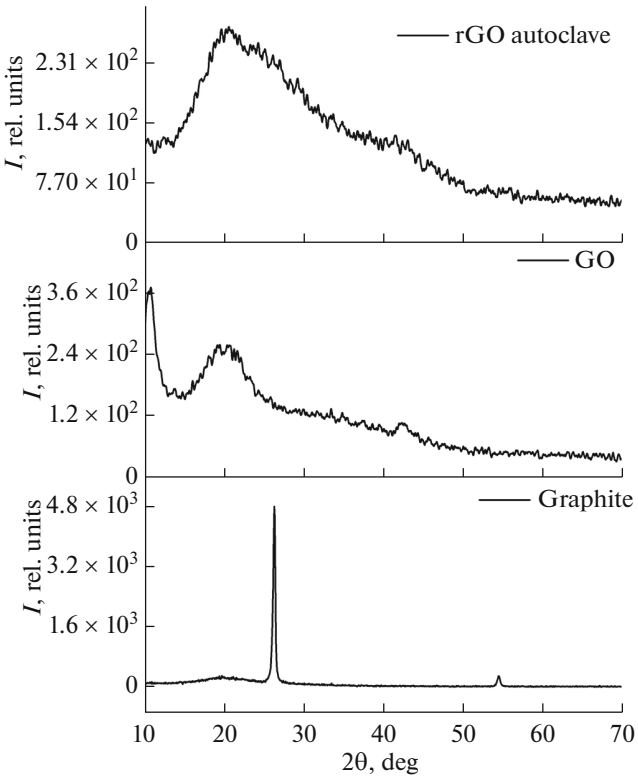

Fig. 2. X-ray diffraction patterns of graphite, graphite oxide, and reduced graphite oxide obtained in an autoclave.

Figure 3 shows the X-ray diffraction patterns of the samples of aerogel and hydrogel based on reduced graphite oxide and gold nanoparticles. The phase compositions of composite hydro- and aerogels are identical. On both roentgenograms, narrow reflections corresponding to gold nanoparticles are clearly visible (angle values 2θ: 38°, 44.5°, 64.6°, and 77.6°, which coincides with the data indicated on card 89-3697, PDF-2) and reflections corresponding to graphite oxide are also present.

Raman-scattering spectroscopy results. Raman spectroscopy is the most widely used method for the analysis of materials based on graphite oxide. The Raman spectra for graphite and its oxide contain *G* and *D* modes in the regions of 1590 and 1340 cm^{-1}, respectively. The intensity of the *D* band increases with the oxidation of graphite to graphite oxide (Fig. 4). The ratio I_D/I_G of the intensities of the components in the spectrum corresponds to the ratio of the sp^2/sp^3 fraction of carbon in the material, which can be considered as a value proportional to the size of the domains of the graphene sheet, while the inverse ratio is a value proportional to the concentration of defects.

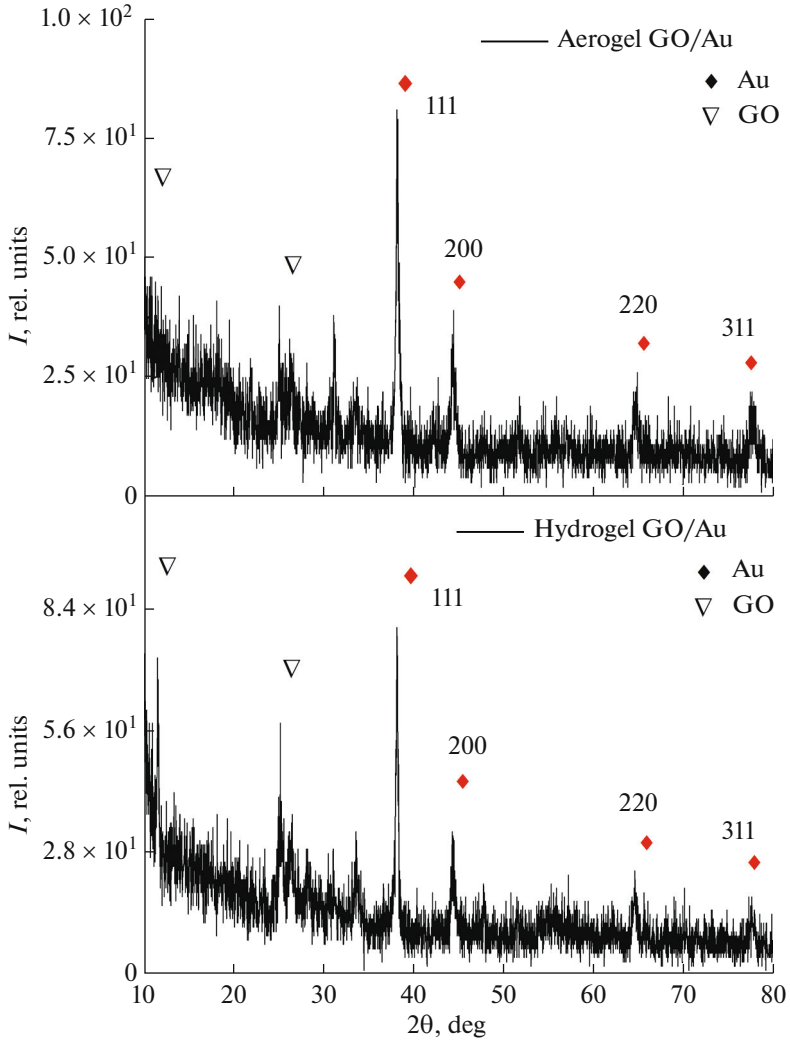

Fig. 3. (Color online) The X-ray diffraction patterns of composite aerogels and hydrogels based on reduced graphite oxide and gold nanoparticles.

For graphite oxide prepared in this work the I_D/I_G ratio is 0.800, which differs significantly from the corresponding value for graphite, 0.213. The formation of a hydro- and aerogel of graphite oxide containing gold nanoparticles is accompanied by a partial reduction of graphite oxide, which is consistent with a decrease in the I_D/I_G ratio to the values of 0.561 and 0.753, respectively (Fig. 4).

Transmission electron microscopy results. The TEM method was used to analyze the microstructure of gold nanoparticles obtained by the Turkevich method and the aerogel based on graphite oxide and gold nanoparticles (Fig. 5).

The obtained gold particles had a spherical shape; the average particle size was 16–18 nm, which is typical for gold nanoparticles obtained by this method. The spherical shape and size of the gold nanoparticles remain unchanged in a composite aerogel.

The results of UV–vis spectroscopy of methylene blue solutions. Construction of a calibration curve. To conduct quantitative experiments on the sorption of a methylene blue (MB) solution by carbon-containing materials, a calibration curve was constructed using the results of UV–vis absorption spectroscopy of MB aqueous solutions with concentrations of 10, 3, 1, 0.3, and 0.1 mg/L. The maximum absorption of MB solutions was observed at a wavelength of 664 nm.

Comparison of the sorption capacity of hydrogel and aerogel based on reduced graphite oxide and gold nanoparticles. An MB solution with a concentration of 10 mg/L was used In sorption experiments.

In order to construct a plot $W(t)$ of the dependence of the sorption efficiency (W) on the contact time of the sorbent with the dye solution (t), the data obtained

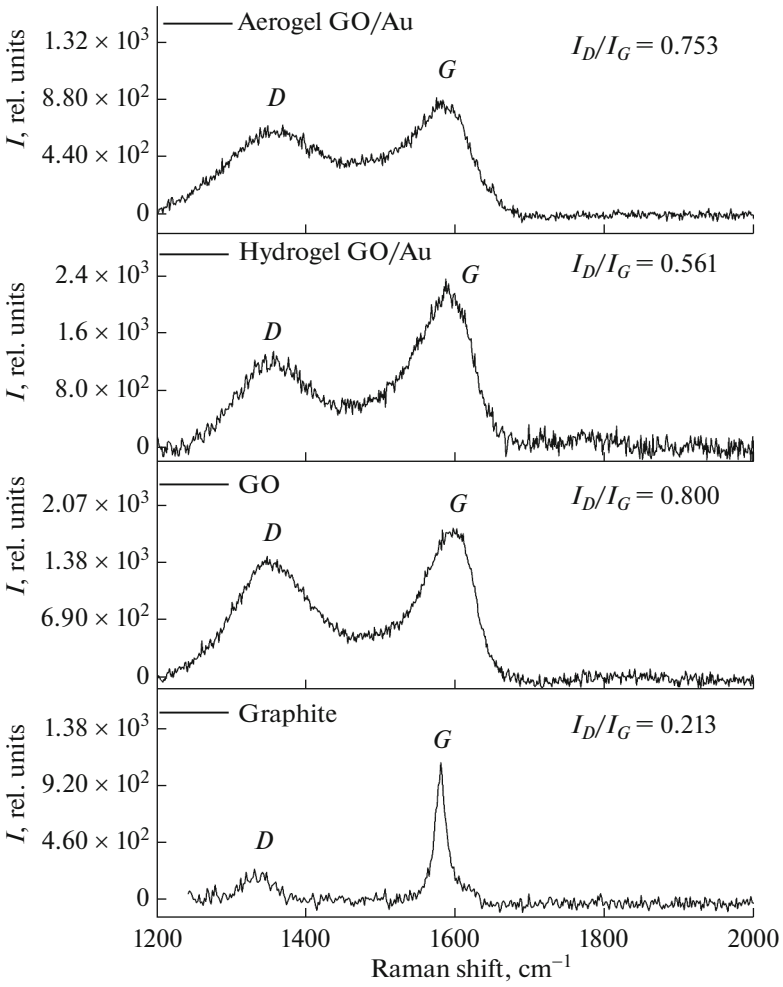

Fig. 4. The Raman spectra for samples of graphite, graphite oxide, hydro- and aerogel based on graphite (laser wavelength 514 nm).

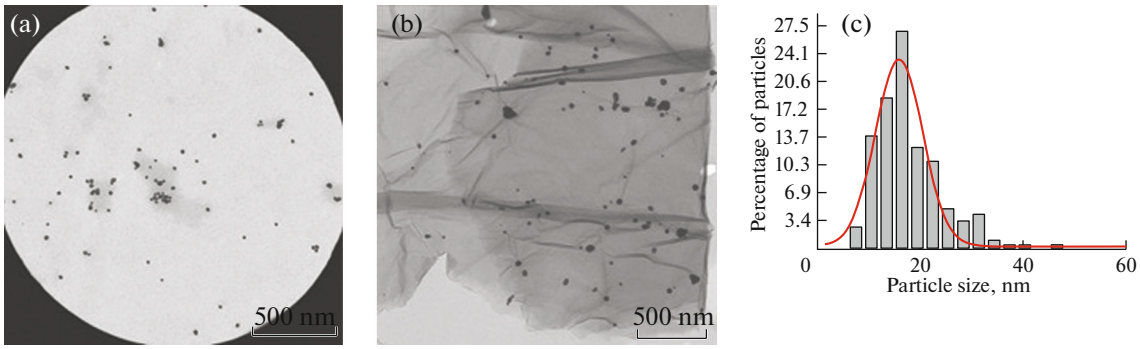

Fig. 5. (Color online) TEM images of (a) gold nanoparticles, (b) an aerogel based on graphite oxide and gold nanoparticles, and (c) a size distribution diagram of gold nanoparticles.

by optical spectroscopy were recalculated according to the equation

$$W = \frac{q_0 - q}{q_0},$$

where q_0 is the optical density of the solution at the initial time and q is the optical density of the solution at a given time.

Figure 6 shows graphs of the dependence of the sorption efficiency on the contact time with a methylene

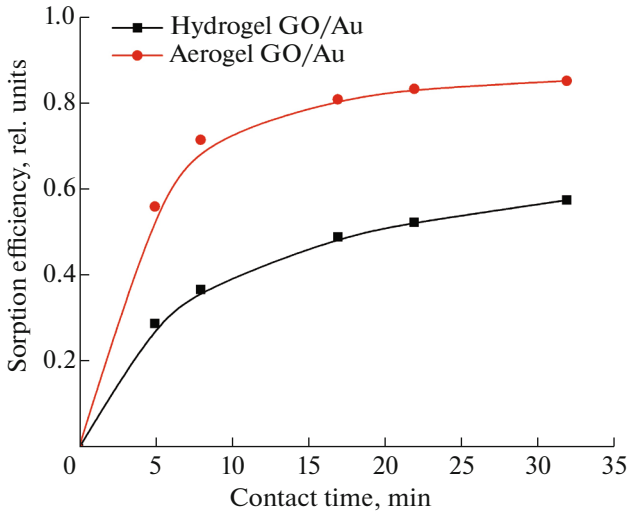

Fig. 6. (Color online) The calibration curve for aqueous methylene blue solutions.

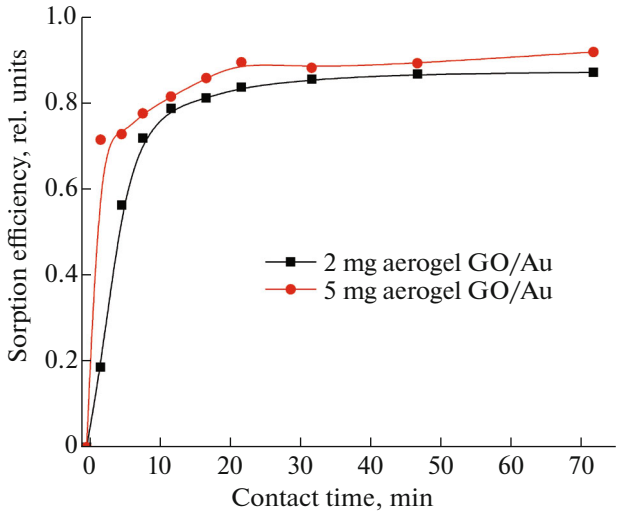

Fig. 7. (Color online) Comparison of the sorption ability of two aerogels rGO–AuNPs.

blue solution for aerogel and hydrogel based on reduced graphite oxide and gold nanoparticles.

From Fig. 6 one can see that the aerogel-based composite sorbs more efficiently (>80%) than the hydrogel-based composite (~50%). This is because the hydrogel contains significant amounts of water, unlike the aerogel, which has a 3D structure with a large number of pores that contributes to the effective sorption of the dye.

Based on the results, all subsequent experiments were carried out with the aerogel based on graphite oxide and gold nanoparticles.

The effect of the amount of sorbent on the efficiency of sorption. To identify the dependence of the sorption efficiency on the sorbent mass, two series of experiments were carried out with different masses of the aerogel based on graphite oxide and gold nanoparticles: 2 and 5 mg. The obtained graphs of the dependence of sorption on time for two series of aerogel samples are presented in Fig. 7.

From Fig. 7 one can see that an increase in sorbent mass contributes to a slight increase in sorption efficiency (92% when using 5 mg rGO–AuNPs and 87% when using 2 mg) and an increase in the rate of the sorption process at the initial stage. For both experiments, the formation of a plateau is observed, which indicates the establishment of equilibrium in the system.

The dependence of sorption on temperature. To study the effect of temperature on the sorption efficiency of a dye solution, two series of experiments were carried out, at 25 and 40°C. As a sorbent, 2 mg rGO–AuNPs were used (Fig. 8).

The data presented in Fig. 8 indicate a decrease in the efficiency of sorption with increase in temperature of the solution of the sorbed dye. This is consistent with the fact that sorption is an exothermic process; therefore, with increase in temperature, the equilibrium shifts toward the endothermic desorption process.

The dependence of the sorption efficiency on the pH value of a dye solution. To study the effect of the pH of the dye solution on the efficiency of sorption, the experiments were carried out in acidic (pH 3), alkaline (pH 10), and neutral (pH 7) media. The pH of the solution was adjusted to the desired value using solutions of hydrochloric acid or potassium hydroxide (Fig. 9).

From the data presented in Fig. 9, one can see that the efficiency of sorption is the largest in a neutral

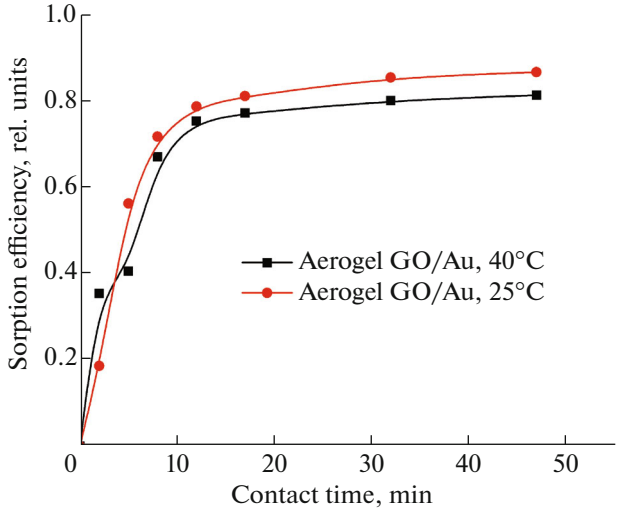

Fig. 8. (Color online) The temperature dependence of the efficiency of sorption.

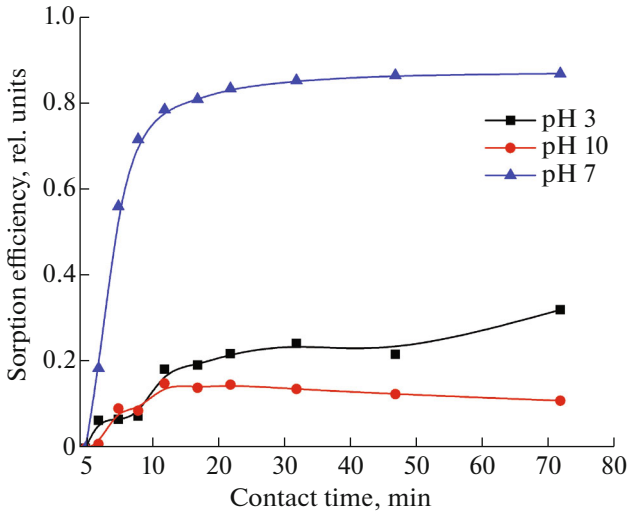

Fig. 9. (Color online) The dependence of the efficiency of sorption on the pH of dye solution.

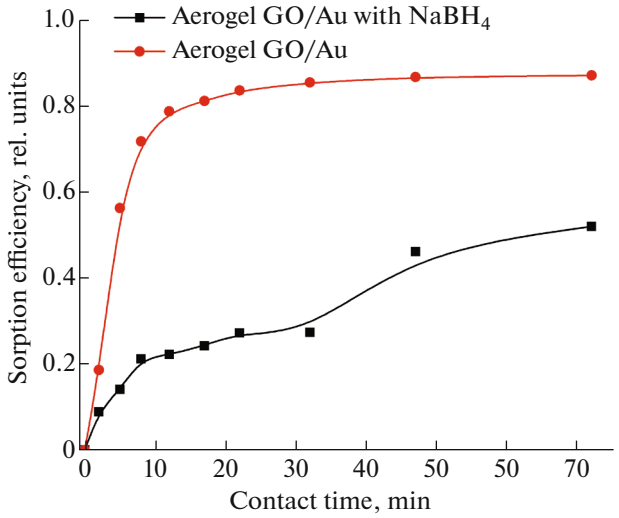

Fig. 10. (Color online) The dependence of sorption on the presence of a reducing agent in the solution.

medium (the maximum sorption is 87%). In acidic and alkaline media the values of maximum sorption efficiency are 32 and 11%, respectively.

The lower efficiency of sorption in an acidic medium compared to a neutral one occurs due to the fact that the nitrogen atom included in the MB molecule can be protonated and acquire a partially positive charge, which will prevent further dye sorption by carboxyl groups on the surface of graphite oxide.

The low sorption ability of aerogels with respect to the MB solution in an alkaline medium can be due to the deprotonation of carboxyl groups on the rGO surface, as a result of which they lose the ability to interact with the N atoms of the dye amino groups.

Thus, aerogels exhibit the best sorption properties in media with neutral pH values.

The dependence of sorption on the presence of a reducing agent in solution. In [21], the authors proposed to carry out sorption of the dye in the presence of $NaBH_4$ in the solution. Therefore, in this work, a series of experiments on the sorption of MB (10 mg/L) was performed in the presence of sodium borohydride (Fig. 10).

The experimental results indicate that the presence of the $NaBH_4$ reducing agent decreases sorption efficiency; the maximum sorption in the presence of sodium borohydride is 52%, while in its absence it was 87%. This is probably caused by the reduction of graphite oxide, in which there is a decrease in the number of oxygen-containing functional groups. This helps to reduce the distance between the layers in the structure and prevents the sorption of the dye.

The dependence of sorption on the presence of gold nanoparticles in the sorbent. To assess the effect of gold nanoparticles on dye sorption processes, we conducted two series of experiments on the sorption of 40 mL of MB solution (10 mg/L) using identical weighed portions (2 mg) of a composite based on reduced graphite oxide and gold nanoparticles and the aerogel based on reduced graphite oxide. The results are presented in Fig. 11.

From the data presented in Fig. 11 one can see that the aerogel based on reduced graphite oxide and gold nanoparticles sorbs slightly better (limiting sorption is 87%) than the aerogel without gold nanoparticles (limiting sorption 75%). Perhaps, this is due to the fact that the gold nanoparticles contained in the aerogel contribute to the destruction of the dye under the action of visible light, which is accompanied by a

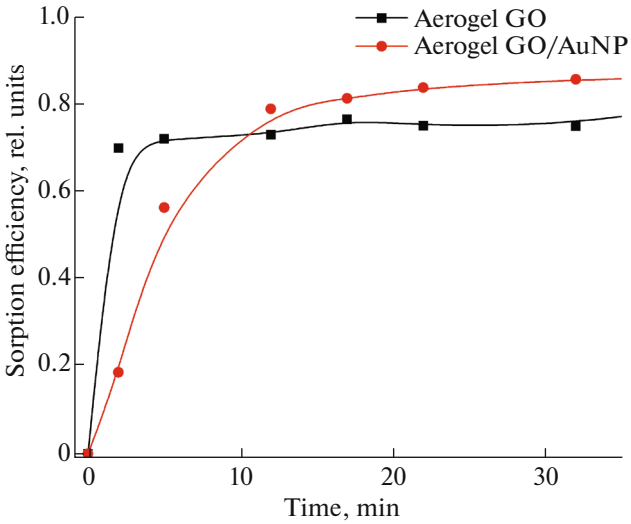

Fig. 11. (Color online) The dependence of sorption on the presence of gold nanoparticles in the sorbent.

change in the color intensity and a decrease in the intensity of the absorption band at 664 nm.

CONCLUSIONS

3D structures based on graphite oxide and gold nanoparticles were synthesized in the form of hydro- and aerogels. Sorption of methylene blue dye solutions was used to characterize the obtained 3D structures. The sorption properties of hydro- and aerogels were compared. The formed porous 3D structure of the aerogel effectively sorbs dye molecules, and the gold nanoparticles included in the composition of the aerogel contribute to dye destruction under the influence of visible light. The dependence of the efficiency of sorption by aerogels on various factors, that is, sorbent mass, acidity of the medium, temperature, and the presence of reducing agents, was studied. It was shown that sorption is efficient when small amounts of aerogels are used, at room temperature, in a neutral environment, and without the use of additional reducing agents. The introduction of gold nanoparticles into aerogels made it possible to increase the sorption efficiency by 15%. These results make it possible to propose aerogels based on graphite oxide and gold nanoparticles as environmentally friendly sorbents for purifying water from dyes that have a harmful effect on the human body and the environment.

FUNDING

This study was supported by the Russian Foundation for Basic Research, project nos. 19-03-00556, 18-29-19120.

REFERENCES

1. A. K. Geim and K. S. Novoselov, "The rise of graphene," Nat. Mater. **6**, 183 (2007).
2. A. Lerf, H. He, M. Forster, and J. Klinowski, "Structure of graphite oxide revisited," J. Phys. Chem. B **102**, 4477 (1998).
3. Yanwu Zhu, Shanthi Murali, Weiwei Cai, et al., "Graphene and graphene oxide: synthesis, properties, and applications," Adv. Mater. **22**, 3906 (2010).
4. H. Gao and H. Duan, "2D and 3D graphene materials: preparation and bioelectrochemical applications," Biosens. Bioelectron. **65**, 404 (2015).
5. B. C. Brodie, "On the athomic weight of graphite," Phil. Trans. R. Soc. London **149**, 249 (1859).
6. W. S. Hammers and R. E. Offeman, "Preparation of graphitic oxide," J. Am. Chem. Soc. **80**, 1339 (1958).
7. D. C. Marcano, D. V. Kosynkin, J. M. Berlin, et al., "Improved synthesis of graphene oxide," ACS Nano **4**, 4806 (2010).
8. I. Kondratowicz, K. Zelechowska, M. Nadolska, et al., "Comprehensive study on graphene hydrogels and aerogels synthesis and their ability of gold nanoparticles adsorption," Colloids Surf. A **528**, 65 (2017).
9. W. Chen and L. Yan, "In situ self-assembly of mild chemical reduction graphene for three-dimensional architectures," Nanoscale **3**, 3132 (2011).
10. Xuan Lu, Xiaoli Liu, Ting Shen, et al., "Convenient fabrication of graphene/gold nanoparticle aerogel as direct electrode for H_2O_2 sensing," Mater. Lett. **207**, 49 (2017).
11. H. Gao and H. Duan, "2D and 3D graphene materials: Preparation and bioelectrochemical applications," Biosens. Bioelectron., No. 65, 404 (2015).
12. Qiangqiang Zhang, Yu Wang, Baoqiang Zhang, et al., "3D superelastic graphene aerogel-nanosheet hybrid hierarchical nanostructures as high-performance supercapacitor electrodes," Carbon, No. 127, 449 (2018).
13. Dong Ma, Jiantao Lin, Yuyun Chen, Wei Xue, Li-Ming Zhang, "In situ gelation and sustained release of an antitumor drug by graphene oxide nanosheets," Carbon **50**, 3001 (2012).
14. E. Jokara, S. Shahrokhiana, A. Iraji zada, et al., "An efficient two-step approach for improvement of graphene aerogel characteristics in preparation of supercapacitor electrodes," J. Energy Storage, No. 17, 465 (2018).
15. Xin Wang, Chengxing Lu, Huifen Peng, et al., "Efficiently dense hierarchical graphene based aerogel electrode for supercapacitors," J. Power Sources, No. 324, 188 (2016).
16. Zh. Sun, W. Fan, and T. Liu, "Graphene/graphene nanoribbon aerogels as tunable three-dimensional framework for efficient hydrogen evolution reaction," Electrochim. Acta, No. 250, 91 (2017).
17. Zh. Yang, G. Xing, P. Hou, and D. Han, "Amino acid-mediated *n*-doped graphene aerogels and its electrochemical properties," Mater. Sci. Eng. B, No. 228, 198 (2018).
18. Xuan Lu, Xiaoli Liu, Ting Shen, et al., "Convenient fabrication of graphene/gold nanoparticle aerogel as direct electrode for H_2O_2 sensing," Mater. Lett., No. 207, 49 (2018).
19. R. Pocklanova, A. K. Rathi, M. B. Gawande, et al., "Gold nanoparticle-decorated graphene oxide: synthesis andapplication in oxidation reactions under benign conditions," J. Mol. Catal. A: Chem. **424**, 121 (2016).
20. Xiaoli Liu, Ting Shen, Zhiyong Zhao et al., "Graphene/gold nanoparticle aerogel electrode for electrochemical sensing of hydrogen peroxide," Mater. Lett. **229**, 368 (2018).
21. J. Xie, X. Yang, and X. Xu, "Wet chemical method for synthesizing 3D graphene/gold nanocomposite: catalytic reduction of methylene blue," Phys. E (Amsterdam, Neth.) **88**, 201 (2017).
22. Yu. V. Ioni, V. V. Voronov, A. V. Naumkin, E. Yu. Buslaeva, A. V. Egorov, S. V. Savilov, and S. P. Gubin, "Platinum, palladium, and rhodium nanoparticles on the surface of graphene flakes," Russ. J. Inorg. Chem. **60**, 709 (2015).
23. Yu. Ioni, E. Buslaeva, and S. Gubin, "Synthesis of graphene with noble metals nanoparticles on its surface," Mater. Today: Proc. **3**, 209 (2016).
24. Fang Ren, Zhen Li, Wen-Zhen Tan, et al., "Facile preparation of 3D regenerated cellulose/graphene oxide composite aerogel with high-efficiency adsorption towards methylene blue," J. Colloid Interface Sci. **532**, 58 (2018).
25. J. Turkevich, P. C. Stevenson, and J. Hillier, "A study of the nucleation and growth processes in the synthesis of colloidal gold," J. Am. Chem. Soc., 55 (1951).

Translated by V. Kudrinskaya